

## Relationship between transpolar flights over the Arctic and the upper atmospheric circulation

Kazutoshi SATO<sup>1</sup> and Jun INOUE<sup>2</sup>

<sup>1</sup>*Kitami Institute of Technology, Kitami, Japan*

<sup>2</sup>*National Institute of Polar Research, Tachikawa, Japan*

(Received October 11, 2018; Revised manuscript accepted December 18, 2018)

### Abstract

International flights from North America to Asia usually take tracks across the Arctic region for reducing fuel and operating costs. For example, the track of United Airlines flight 895 (UAL895) traveling from Chicago to Hong Kong via the Arctic region usually uses the following three routes: the Atlantic, central Arctic, and Pacific routes. Using a reanalysis product, we show that flight routes depend on the location and strength of the upper flow over the Arctic Ocean, which has a seasonal variation. During summer, when anticyclonic flow associated with blocking occurs over the Pacific Arctic region, UAL895 flights choose the Pacific and Atlantic routes to avoid a strong head wind. In addition, when the jet stream is strong over the Atlantic–Arctic region (the northern parts of Greenland and Barents Seas), the Atlantic route is selected to take advantage of strong tail winds resulting from the blocking over this region. During winter and, especially, years with less sea ice in the Bering Sea, the frequency of Alaskan blocking has increased, indicating that the prediction of the sea-ice extent over the Bering Sea would provide useful information for aircraft operation over the Arctic region.

**Key words:** Arctic flight track, sea-ice extent, blocking events

### 1. Introduction

Aircrafts contribute to the emissions of carbon dioxide (CO<sub>2</sub>), water vapor (H<sub>2</sub>O) and oxides of nitrogen, leading to global climate change (Lee and others 2009; 2010). Aircraft CO<sub>2</sub> emissions have increased to 2.5% of the total anthropogenic emitted CO<sub>2</sub> over the previous 50 years (Lee and others 2009). The strengthened column-averaged, north–south temperature-gradient response to the increase in CO<sub>2</sub> has caused an increased level of upper-level clear-air turbulence, which is a major cause of aviation incidents (e.g., injured passengers, structural damage, flight delays) (Sharman and others 2006). Previous studies have reported an increase in the frequency and intensity of turbulence at upper levels for a doubling of the CO<sub>2</sub> concentration (Williams and Joshi 2013, Williams and others 2017, Storer and others 2017). A reduction in fuel usage would, therefore, help to reduce operating costs and minimize climate impacts.

Two approaches to reduce aircraft emissions are the development of technologies (e.g., efficient engines, clean fuels, body and wing forms) and the improvement of air-traffic management (e.g., shortening flight times), which may be optimized by monitoring the upper atmospheric circulation, because aircraft routes and flight lengths mainly depend on the horizontal wind speed at upper levels (Palopo and others 2010).

Therefore, avoiding headwinds and enhancing the probability of tailwinds would reduce aircraft fuel consumption. Previous studies have reported that the change in the phase of atmospheric circulation over the Atlantic sector causes changes in the position and strength of the jet stream, and thereby influences aircraft routes (Irvine and others 2013; Kim and others 2016; Williams 2016). Kim and others (2016) indicated certain links between the route and travel time of a flight from New York to London and the phase of the North Atlantic Oscillation (NAO). In the positive phase (NAO+), when the jet stream tends to shift northward over the northern Atlantic Ocean, flight times become shorter than during the negative phase (NAO-). In addition, the number and timing of the route varies with the season because of differences in the strength and location of the jet stream in summer and winter (Irvine and others 2013). In contrast, over the Pacific Ocean, changes in atmospheric circulation over high and low latitudes (e.g., resulting from the Arctic and El Niño Southern Oscillations) affect the flight time of aircraft at mid-latitudes (Karnauskas and others 2015). Therefore, the route and season are strongly influenced by atmospheric circulation patterns over the Northern Hemisphere.

Polar routes exist to minimize the total travel time and fuel consumption of aircraft travelling from one

continent to another. The commencement of cross-polar flight began in 1998 when entry into Russian airspace was permitted by the Russian Government (Jacobson and others 2011). The number of international flights that use the Arctic route has been increasing in recent decades, with several companies currently using the cross-polar flight track throughout the year.

The United Airlines (UAL) flight 895 travels from Chicago (ORD) to Hong Kong (HKG) almost every day, which, to minimize the distance and time of flight, passes over the Arctic region (Fig. 1a). However, flight UAL895 does not always travel the shortest route from ORD to HKG, suggesting the dependence of the Arctic route on the upper level flow over the Arctic Ocean. We investigate here the relationship between the flight track and the upper-level atmospheric circulation, particularly during the summer and winter seasons.

## 2. Data and methodology

### 2.1 Meteorological data

We use 6-h ERA-Interim reanalysis data from January 1979 to December 2016 on a  $0.75^\circ \times 0.75^\circ$  latitude/longitude grid produced by the European Centre for Medium-Range Weather Forecasts (Dee and others 2011) for determination of the geopotential height, wind speed, sea-surface temperature, and sea-ice concentration. We mainly focus on the atmospheric circulations during summer (from May to August, hereafter MJJA) and winter (from December to March, hereafter DJFM). To calculate the frequency of blocking events over the Northern Hemisphere, we apply a blocking index defined by D'Andrea and others (1998). At each longitude, the meridional gradient of geopotential height at 250 hPa ( $Z_{250}$ ) between the southern and northern parts of  $Z_{250}$  ( $GHGS$  and  $GHGN$ ) are calculated as

$$GHGS = Z(\psi_0) - Z(\psi_s) / (\psi_0 - \psi_s) \quad (1)$$

and

$$GHGN = Z(\psi_n) - Z(\psi_0) / (\psi_n - \psi_0) \quad (2)$$

respectively, where

$$\begin{aligned} \psi_n &= 76.5^\circ \pm \Delta \\ \psi_0 &= 60.0^\circ \pm \Delta \\ \psi_s &= 43.5^\circ \pm \Delta \end{aligned} \quad (3)$$

for  $\Delta = 0^\circ, 0.75^\circ, 1.5^\circ, 2.25^\circ, 3.0^\circ, 3.75^\circ, 4.5^\circ$ .

A specific longitude on a given day is locally defined as being blocked if both of the following conditions are satisfied (for at least one value of  $\Delta$ ):

$$GHGS > 0 \quad (4)$$

and

$$GHGN < -5 \text{ m/}(\text{degrees latitude}) \quad (5)$$

(a) UAL 895 flight routes

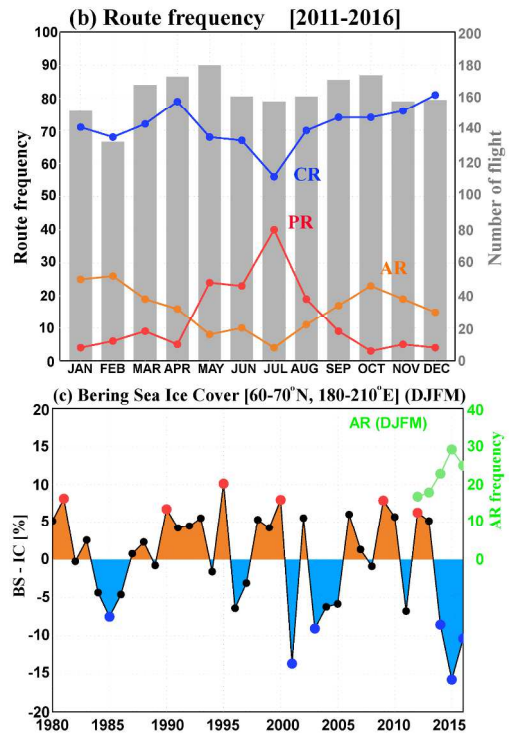
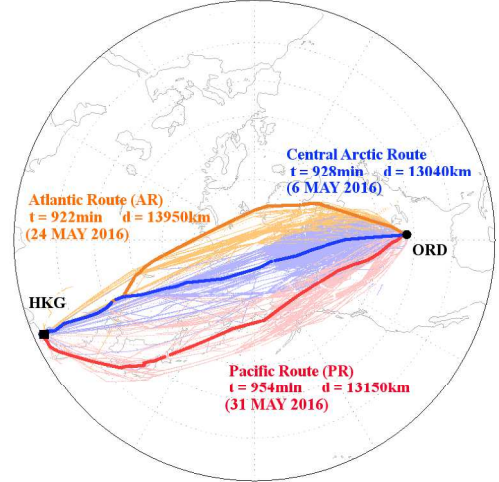


Fig. 1 (a) All flight tracks (thin lines) and the representative track (thick lines) for the Atlantic (AR, orange), central Arctic (CR, blue) and Pacific routes (PR, red) for May 2016. The time and distance for the representative tracks are shown.

(b) Monthly average frequency of each route from 2011–2016. Gray bars show the number of flights from Chicago (ORD) to Hong Kong (HKG) via the Arctic region from 2011–2016.

(c) Ice-cover anomaly during December and March from the climatology over the Bering Sea ( $60\text{--}70^\circ\text{N}$ ,  $180\text{--}210^\circ\text{E}$ ) from ERA-Interim. The green line shows the frequency of flights taking the Atlantic route.

### 2.2 Flight track data

Flight information is obtained from the flightaware website (<https://flightaware.com>), which provides the location, height and total flight time of commercial flights all over the world. We focus on flight UAL895

from ORD to HKG over the Arctic region (Fig. 1a), whose average total flight time is about 16 h depending on the flight track. Flight information is available since 2011, which is a relatively long time period compared with other flights for this route.

We use the northernmost position of aircraft over the Atlantic (15°W–15°E) and Pacific (165°E–165°W) Arctic regions to classify UAL895 flight tracks, resulting in three routes: the Atlantic route (northward of 75°N over the Atlantic–Arctic region or northward of 87°N over the Pacific–Arctic region), the central Arctic route (from 72°N to 87°N over the Pacific–Arctic region) and the Pacific route (southward of 72°N over the Pacific–Arctic region). Examples of flight tracks for each route in May 2016 are shown in Fig. 1(a). As the central Arctic route is the most efficient and shortest route between ORD and HKG, it is the most common of the three routes throughout the year (Fig. 1(b)). Both the Atlantic and Pacific routes have a longer distance compared with the central Arctic route, however, flight UAL895 sometimes chooses them at a frequency depending on the season. While the Pacific route has a higher frequency during MJJA, the Atlantic route has a higher frequency during DJFM, indicating that the aircraft routing over the Arctic region depends on the atmospheric circulation and season.

### 3. Relationship between the Arctic flight route and upper-atmospheric circulation

#### 3.1 Summer

During summer, flight UAL895 chooses the central Arctic or Pacific routes almost exclusively (Fig. 1(b)). To understand the difference in upper atmospheric circulation patterns between the central Arctic and Pacific routes, we constructed maps of geopotential height and wind speed at 250 hPa (Z250 and W250) by subtracting the composites of central-Arctic-route days from those of Pacific-route days during summer. Figure 2(a) shows the differences in Z250 and W250 between the Pacific- and central-Arctic-route days during summer, with positive anomalies of Z250 found over the Pacific–Arctic sector. The head-wind anomalies from far eastern Eurasia to the Canadian Arctic Archipelago are consistent with an anticyclone flow associated with positive Z250 anomalies. In contrast, the tail-wind anomalies associated with positive Z250 anomalies are seen from eastern Asia to Canada. Therefore, the Pacific route is very favorable for flight UAL895 when the head wind over the Pacific–Arctic region is strengthened, and the tail-wind anomaly is strong from Alaska to eastern Asia.

The positive anomalies of Z250 suggest the increase in the frequency of summer blocking over eastern Asia and the Beaufort Sea during Pacific-route days. The peak blocking events over the European–Atlantic and Pacific regions are significant weather events according

to previous studies (Matsueda 2009, Matsueda and Endo 2017, Hoffman and others 2014). We show the difference in the frequency of summer blocking events between the central-Arctic-route and Pacific-route days in Fig. 3(a), where, over the Pacific region (around 150°E and 130°W), two peaks of the difference in the frequency of blocking are clearly seen. The increases in the blocking frequency are consistent with a positive Z250 anomaly over eastern Asia and Alaska/northern Canada (Fig. 2(a)). When the blocking dominates over the Pacific–Arctic region, flight UAL895 takes the Pacific route to avoid the strong head wind associated with this blocking pattern. This result suggests that the blocking events over the Pacific–Arctic regions and eastern Asia are the fundamental phenomena governing flight routes during summer.

#### 3.2 Winter

We focus on the difference in atmospheric circulation between the central Arctic and Atlantic routes, where the latter is more frequent during winter (Fig. 1(b)). Using the same composite maps as in Fig. 2(a), but focusing on the winter case (Fig. 2(b)), we see that for Atlantic-route days, positive Z250 anomalies appear over Alaska and western Canada, causing head-wind anomalies from the central Arctic to the Canadian Arctic Archipelago. In contrast, tail-wind anomalies exist from northern Greenland to central Siberia. The positive Z250 anomaly dominates over the Barents Sea, enhancing anticyclonic flow at the upper level. For Pacific-route days, positive Z250 anomalies are found over Alaska and western Canada, however, a positive W250 anomaly is not clearly seen over the Barents Sea (not shown).

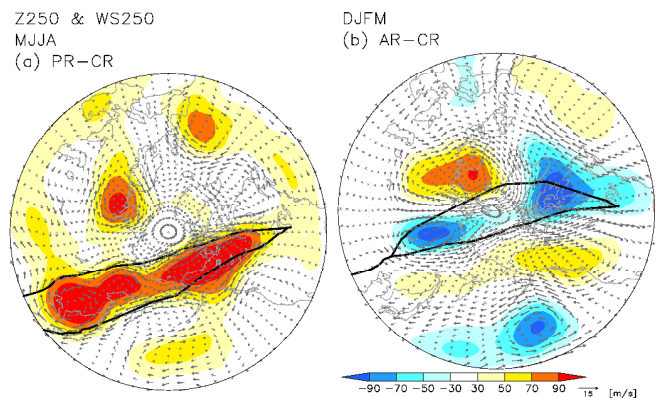


Fig. 2 (a) Difference maps in geopotential height (Z250 [m]: shading) and air velocity (vectors [m/s]) at 250 hPa between the Pacific (PR) and central Arctic (CR) routes for summer (MJJA).

(b) Difference maps in geopotential height (shading [m]) and velocity (vectors [m/s]) at 250 hPa between the Atlantic (AR) and central Arctic routes for winter (DJFM). Black contours show the representative tracks as shown in Fig. 1a.

During winter, relatively higher blocking frequencies are found over the European–Atlantic and Pacific sectors for Atlantic-route and central-Arctic days. There is a difference in blocking frequencies over the European–Atlantic sector (between 20°E and 50°E) and the Pacific region (between 150°E and 130°W) in winter (Fig. 3b), although the amplitude of difference is smaller than that in summer. The peak European–Atlantic (Pacific) blocking difference results from a positive anomaly of Z250 over the Barents Sea (from Alaska to western Canada), suggesting that the winter blocking over the Pacific and European–Atlantic sectors impacts the aircraft route over the Arctic Ocean.

### 3.3 Atmospheric response to change in Arctic sea ice

The decline in Arctic winter sea ice promotes turbulent heat release into the atmosphere, resulting in a geopotential height anomaly over the Arctic region (Rinke and others 2013). To understand the atmospheric response to sea-ice decline over the Arctic, we focus on years with low and high sea-ice extent in the Bering Sea (Fig. 1(c)), and investigate the difference in the atmospheric circulation in Z250 fields during winter (Fig. 4(a)). The Z250 anomaly pattern is similar that for Atlantic-route days as shown in Fig. 2(b), particularly for the Western Hemisphere, indicating that this anomaly pattern may be a response to the decline in Bering Sea ice. In fact, the frequency of Atlantic-route days during winter was relatively high during years of low ice extent (the winters of 2015 and 2016), while in years with a high ice extent (the winters of 2012 and 2013), the frequency was relatively low compared with other years. To investigate the relationship between the sea-ice extent over the Bering Sea and the atmospheric circulation over the Northern Hemisphere, we performed regression analyses between Z250 and the sea-ice concentration over the Bering Sea (Fig. 4(b)), giving a positive correlation over western Canada and a negative correlation over the North Pacific. This pattern of Z250 is similar to patterns of the Z250 anomaly during years with a low ice extent (Fig. 4(a)) and Atlantic-route days (Fig. 2(b)), although the amplitude of Z250 is smaller than for Z250 anomalies in Figs. 2(b) and 4(a), indicating that the increased Alaskan blocking frequency during years with a low ice extent influences flight operations.

For composite maps as in Fig. 4(a), but focusing on the summer case, the Z250 anomaly pattern is different from the winter case in terms of the atmospheric response to sea-ice decline over the Bering Sea (not shown), because anomalous snow melting in northern Eurasia leads to summer atmospheric circulation anomalies (Matsumura and others 2010). Matsumura and Yamazaki (2012) found that large surface heating associated with early snow melting in northern Eurasia

forms an anticyclonic circulation anomaly over eastern Siberia. In addition, the El Niño–Southern Oscillation and the development of the Okhotsk High determine the degree of summer blocking over the eastern Asia region (Park and Ahn 2014).

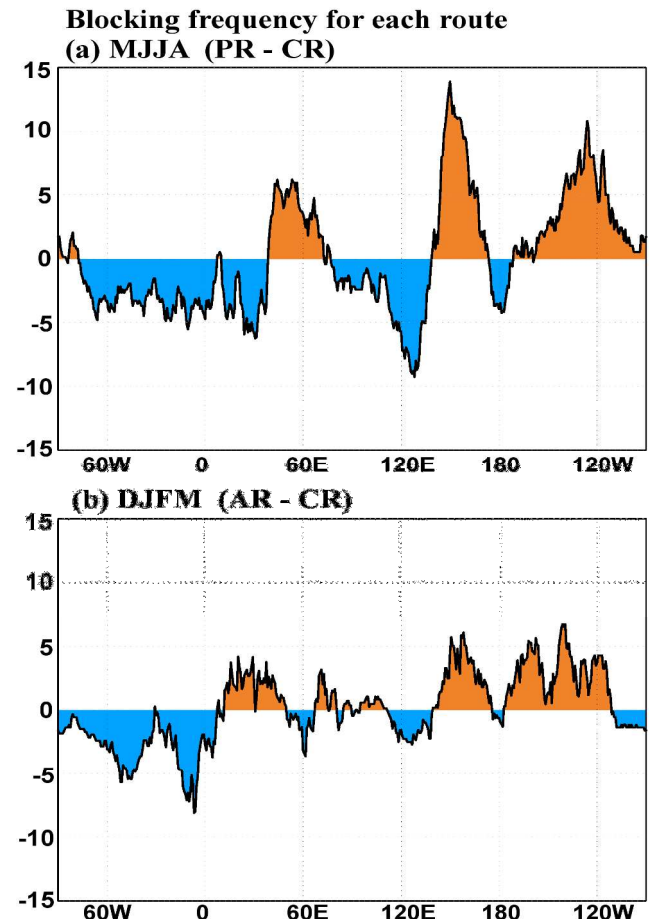


Fig. 3 (a) Difference in frequency of blocking [%] between the Pacific (PR) and central Arctic (CR) routes (PR-CR) in summer (MJJA) as a function of longitude.

(b) Difference in frequency of blocking [%] between the Atlantic (AR) and central Arctic (CR) routes (AR-CR) in winter (DJFM) as a function of longitude.

## 4. Summary and discussion

We have investigated the relationship between the upper level flow over the Northern Hemisphere and flight tracks over the Arctic region. The tail wind anomaly from northern Greenland to western Siberia is induced by European–Atlantic blocking, which influences flight operations during winter. Alaskan blocking events during summer, which result in a head-wind anomaly from eastern Siberia to the Canadian Arctic Archipelago, impede aircraft from crossing the central Arctic route, while the tail wind anomaly from Alaska to eastern Asia is favorable for the Pacific route. Our composite analysis demonstrates the impact of blocking events on aircraft routes.

However, operational and fuel costs must be discussed before the beneficial operation of flights can be considered. Operational costs not discussed here include the cost of entering another country's airspace, which differs for each country. Previous studies have reported that the increased probability of a tail wind minimizes the total flight time, and reduces the fuel and operational costs (Williams 2016, Karnauskas and others 2016, Kim and others 2016). Based on results of these studies, using the tail wind anomaly from northern Greenland to western Siberia and over the Pacific Ocean, while avoiding the head wind anomaly area from eastern Siberia to the Canadian Arctic Archipelago, would reduce operational and fuel costs. Hence, the accurate forecast of blocking events is important for aircraft operation over the Arctic region.

The frequency of summer Pacific blocking events from 2051 and 2110 is expected to increase slightly (Matsueda and Endo 2017). In addition, Pacific blocking events lasting 15–29 days are predicted to increase in the future, suggesting that planning would be simplified because once a blocking situation develops, the atmospheric pattern likely persists for weeks, which favors the Pacific route. In contrast, winter blocking events lasting 9 days or less are expected to increase in the future. Our results show that the frequency of the Alaskan blocking event is related to the sea-ice concentration over the Bering Sea, and would be the determining factor during years with a low sea-ice extent in the Bering Sea. An accelerated decline in the Arctic sea ice would lead to an increase in the frequency of Alaskan blocking events, which would continue to influence aircraft operation over the Arctic region in the future.

As the sea-ice retreat in the Bering Sea is predictable through the 3-month leading Z500 (Nakanowatari and others 2015), the forecasting of sea-ice variability would provide an efficient guide for aircraft operations over the Arctic Ocean. However, the amplitude of the Z250 anomaly associated with sea-ice decline is smaller than that of the difference in Z250 between years with a low and high ice extent, implying that the Z250 anomaly is not entirely explained by the decline in Arctic sea ice. For example, the change in sea-surface temperature over the mid-latitudes has a large impact on storm tracks in the Northern Hemisphere, resulting in a wind-speed anomaly over the Arctic region (Sato and others 2014, Ok and others 2017). Screen and Francis (2014) suggested that the atmospheric response to the variability of sea-surface temperature over tropical ocean causes the wind-speed and temperature anomalies at higher latitudes. Therefore, sensitivity experiments must be performed to investigate the atmospheric response to a change in the sea-surface temperature over mid-latitudes and the tropics in the near future.

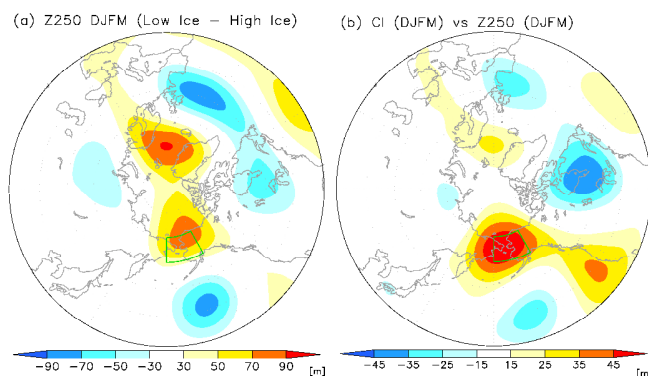


Fig. 4 (a) Difference maps in Z250 between years with low and high sea-ice extent in the Bering Sea for winter (DJFM).

(b) Regression field of Z250 with Bering Sea ice cover in winter.

### Acknowledgements

This work was supported by a Grant-in-Aid for Scientific Research (KAKENHI(A) 18H03745) and the Arctic Challenge for Sustainability (ArCS) project. We would like to thank anonymous reviewers whose constructive comments improved the quality of this manuscript. We used United Airline 895 flight information from Flightaware (<https://flightaware.com>). We thank Richard Foreman, PhD, from Edanz Group ([www.edanzediting.com/ac](http://www.edanzediting.com/ac)) for correcting a draft of this manuscript.

### References

- D'Andrea F., and 16 others (1998): Northern Hemisphere atmospheric blocking as simulated by 15 atmospheric general circulation models in the period 1979–1988. *Clim. Dyn.*, **14**, 385–407, doi:10.1007/s003820050230.
- Dee, D.P. and 35 others (2011): The ERA-Interim reanalysis: configuration and performance of the data assimilation system, *Q. J. R. Meteorol. Soc.*, **137**, 553–597.
- Hoffman, H.N. and W. Zhou (2014): Implications of Ural blocking for East Asia winter climate in CMIP5 GCMs. Part I: Biases in the historical scenario, *J. Clim.*, **28**, 2203–2216, doi: 10.1175/JCLI-D-14-00308.1.
- Irvine, E. A., B.J. Hoskins, K.P. Shine, R.W. Lunnon and C. Froemming (2013): Characterizing North Atlantic weather patterns for climate-optimal aircraft routing, *Meteorol. Appl.*, **20**, 80–93.
- Jacobson, M.Z., J.T. Wilkerson, S. Balasubramanian, W.W.Jr. Cooper and N. Mohleji (2012): The effects of rerouting aircraft around the arctic circle on arctic and global climate, *Climatic Change*, **115**, 709–724, doi:10.1007/s10584-012-0462-0.
- Karnauskas, K.B., J.P. Donnelly, H.C. Barkley and J.E. Martin (2015): Coupling between air travel and climate, *Nat. Clim. Change*, **5**, 1068–73.
- Kim, J.-H., W.N. Chan, B. Sridhar, R.D. Sharman, P.D. Williams and M. Strahan (2016): Impact of the North Atlantic Oscillation on transatlantic flight routes and clear-air turbulence, *J. Appl. Meteor. Climatol.*, **55**, 763–771.
- Lee, D.S., D.W. Fahey, P.M. Forster, P.J. Newton, R.C.N. Wit, L.L. Lim, B. Owen and R. Sausen (2009): Aviation and global climate change in the 21st century, *Atmos. Environ.*, **43**, 3520–3537.

- Lee, D. S., G.Pitari, V. Grewe, K. Gierens, J.E. Penner, A. Petzold, M.J. Prather, U. Schumann, A. Bais, T. Berntsen, D. Iachetti, L.L. Lim and R. Sausen (2010): Transport impacts on atmosphere and climate: aviation, *Atmos. Environ.*, **44**, 4678–4734.
- Matsueda, M. (2009): Blocking predictability in operational mediumrange ensemble forecasts, *SOLA*, **5**, 113–116.
- Matsueda, M. and H. Endo (2017): The robustness of future changes in Northern Hemisphere blocking: A large ensemble projection with multiple sea surface temperature patterns *Geophys. Res. Lett.*, **44**, 5158–5166, doi:10.1002/2017GL073336.
- Matsumura, S., K. Yamazaki and T. Tokioka (2010): Summertime landatmosphere interactions in response to anomalous springtime snow cover in northern Eurasia, *J. Geophys. Res.*, **115**, D20107, doi :10.1029/2009JD-12342.
- Matsumura, S. and K. Yamazaki, (2012): Eurasian subarctic summer climate in response to anomalous snow cover, *J. Clim.*, **25**, 1305–1317.
- Nakanowatari, T., J. Inoue, K. Sato and T. Kikuchi (2015): Summertime atmosphere-ocean preconditionings for the Bering Sea ice retreat and the following severe winters in North America, *Environ. Res. Lett.*, **10**, 094023, doi: 10.1088/1748-9326/10/9/094023.
- Ok, J., M.K. Sung, K. Sato, Y.K. Lim, S.J. Kim, E.H. Baek, J.H. Jeong and B.M. Kim (2017): How does the SST variability over the western North Atlantic Ocean control Arctic warming over the Barents/Kara seas? *Environ. Res. Lett.*, **12**, 034021.
- Palopo, K., R.D. Windhorst, S. Suharwardy and H.-T. Lee (2010): Windoptimal routing in the national airspace system, *J. Aircr.*, **47**, 1584–1589.
- Park, Y.J. and J.B. Ahn, (2014): Characteristics of atmospheric circulation over East Asia associated with summer blocking *J. Geophys. Res. Atmos.*, **119**, 726–738, doi:10.1002/2013JD020688.
- Rinke, A., K. Dethloff, W. Dorn, D. Handorf and J.C Moore (2013): Simulated Arctic atmospheric feedbacks associated with late summer sea ice anomalies, *J. Geophys. Res.*, **118**, 7698–7714.
- Sato, K., J. Inoue and M. Watanabe (2014): Influence of the Gulf Stream on the Barents Sea ice retreat and Eurasian coldness during early winter, *Environ. Res. Lett.*, **9**, 084009, doi:10.1088/1748-9326/9/8/084009.
- Screen, J.A. and J.A. Francis (2016): Contribution of sea-ice loss to Arctic amplification is regulated by Pacific Ocean decadal variability, *Nat. Clim. Change*, **6**, 856–860.
- Sharman, R., C. Tebaldi, G. Wiener and J. Wolff, (2006): An integrated approach to mid- and upper-level turbulence forecasting, *Weather Forecast*, **21**, 268–287.
- Storer, L.N., P.D. Williams and M.M. Joshi, (2017): Global response of clear-air turbulence to climate change, *Geophys. Res. Lett.*, **44**, 9976–9984, doi:10.1002/2017GL074618.
- Williams, P.D. and M.M Joshi (2013): Intensification of winter transatlantic aviation turbulence in response to climate change, *Nat. Clim. Change*, **3**, 644–648.
- Williams, P. D. (2016): Transatlantic flight times and climate change, *Environ. Res. Lett.*, **11**, 024008, doi: 10.1088/1748-9326/11/2/024008.
- Williams, P.D. (2017): Increased light, moderate, and severe clear-air turbulence in response to climate change. *Adv. Atmos. Sci.*, **34**(5), 576–586, doi: 10.1007/s00376-017-6268-2.

## Summary in Japanese

和文要約

### 北極海空路と北半球の大気循環場との関係

佐藤和敏<sup>1</sup>, 猪上淳<sup>2</sup>

<sup>1</sup>北見工業大学, <sup>2</sup>国立極地研究所

北アメリカ-アジア間で運行されている国際線は、エネルギー消費や飛行時間を抑えるため、距離の短くなる北極海の上空を通過する。シカゴ-香港間で運行されているユナイテッド航空 895 便(UAL895)は、北極海の上空を通過する航空機の1つだが、北極海上を通過する空路は主に 3 つ(太平洋側ルート、中央北極海ルート、大西洋側ルート)に分類することができる。これは、飛行機は上空の追い風を受けることで、飛行時間を短縮できるためである。そこで本研究では、再解析データを用いて、北半球のブロッキングに伴う風の強さや位置の変化と UAL895 が北極海上を飛行するルートに関係があることを明らかにした。北半球では、ブロッキングに伴い北極海太平洋側で高気圧性の循環が強まると、北極海中央で向かい風が強くなるため、航空機が北極海の大西洋側や太平洋を通過する傾向にある。一方、大西洋側北極海でブロッキングに伴い上空の風が強まると、グリーンランド上空で追い風が強くなるため、大西洋側北極海を通過する傾向にあった。北極海の上空の大気循環は、熱帯の海面水温やベーリング海の海氷分布と関係性が見られており、数ヶ月前から予報可能であることが示唆され、北極海ルートを通過する航空会社に有益な情報を提供できる可能性がある。

Copyright ©2019 The Okhotsk Sea & Polar Oceans Research Association. All rights reserved.